New *ab initio* potential energy surface and the vibration-rotation-tunneling levels of $(H_2O)_2$ and $(D_2O)_2$

X. Huang,[a] Bastiaan J. Braams, and Joel M. Bowman[b]
Cherry L. Emerson Center for Scientific Computation, Department of Chemistry, Emory University, Atlanta Georgia 30322, USA

Ross E. A. Kelly and Jonathan Tennyson
Department of Physics and Astronomy, University College London, Gower St., London WC1E 6BT, United Kingdom

Gerrit C. Groenenboom and Ad van der Avoird[c]
Theoretical Chemistry, Institute for Molecules and Materials, Radboud University Nijmegen, Toernooiveld 1, 6525 ED Nijmegen, The Netherlands

(Received 13 September 2007; accepted 14 November 2007; published online 18 January 2008)

We report a new full-dimensional potential energy surface (PES) for the water dimer, based on fitting energies at roughly 30 000 configurations obtained with the coupled-cluster single and double, and perturbative treatment of triple excitations method using an augmented, correlation consistent, polarized triple zeta basis set. A global dipole moment surface based on Møller-Plesset perturbation theory results at these configurations is also reported. The PES is used in rigorous quantum calculations of intermolecular vibrational frequencies, tunneling splittings, and rotational constants for $(H_2O)_2$ and $(D_2O)_2$, using the rigid monomer approximation. Agreement with experiment is excellent and is at the highest level reported to date. The validity of this approximation is examined by comparing tunneling barriers within that model with those from fully relaxed calculations. © *2008 American Institute of Physics*. [DOI: 10.1063/1.2822115]

I. INTRODUCTION

The water dimer is of central importance as a key building block for models of liquid water and ice. In its own right it is of fundamental interest as it exhibits large-amplitude, internal hydrogen bond rearrangements. High-resolution microwave and far-infrared spectroscopy has determined the tunneling splittings associated with these rearrangements.[1–9] These provide vital and challenging data for theorists to understand and reproduce with high-quality potentials for the dimer and realistic quantum calculations of the tunneling using such potentials. There has been great progress in realizing this goal recently.[10] Here, we report additional and significant progress in this effort.

Previously, three of us (X.H., B.B., and J.B.) reported a full-dimensional global potential energy surface (PES) for $(H_2O)_2$ based on roughly 20 000 *ab initio* energies using the CCSD(T) method with an aug-cc-pVTZ basis.[11] The properties of this PES were extensively reviewed and shown to be quite accurate compared to previous *ab initio* calculations done at all known stationary points. Here, we report a new potential energy surface and dipole moment surface (DMS) that is based on an additional 10 000 configurations which significantly improve the accuracy of the previous PES at energies below 10 000 cm^{-1} above the global minimum. We label this new potential as "HBB" where "HBB" refers to three of the authors, Huang, Braams, and Bowman, and the previous one as "HBB0." The potential (like the previous one) is manifestly invariant with respect to all permutations of like nuclei. The properties of this new PES and DMS are presented. The PES is used in six-dimensional (6D), rigid monomer calculations of the vibration-rotation-tunneling (VRT) levels of $(H_2O)_2$ and $(D_2O)_2$ using the code developed by Groenenboom *et al.*[12] The VRT levels are compared to results from high-resolution teraherz spectroscopy, and excellent agreement is found.

The paper is organized as follows. The construction and properties of the new HBB PES are presented in the next section, followed by a brief description of the methods used to calculate the low-lying VRT states of $(H_2O)_2$ and $(D_2O)_2$ in Sec. III. The results of those calculations using the HBB PES are discussed and compared with experiment in the second part of that section. The discussion includes some comments on the possible effects of nonrigidity. A brief summary and conclusions are given in Sec. IV.

II. *AB INITIO* POTENTIAL ENERGY SURFACE

The HBB PES is a fit to roughly 30 000 *ab initio* energies obtained with the coupled-cluster method including singles and doubles and a perturbative correction for triples [CCSD(T)] using an aug-cc-pVTZ basis as implemented in MOLPRO.[13] Of these 30 000 energies roughly 20 000 were used in our previous HBB0 PES.[11] The distribution of those 20 000 energies was described in detail previously. In brief fourteen OO distances were selected from 4 to 100 bohrs, with eight distances between 4 and 6 bohrs, four between 8

[a]Mail stop: 245-6, NASA Ames Research Center, Moffett Field, California 94035, USA.
[b]Electronic mail: jmbowma@emory.edu.
[c]Electronic mail: A.vanderAvoird@theochem.ru.nl.

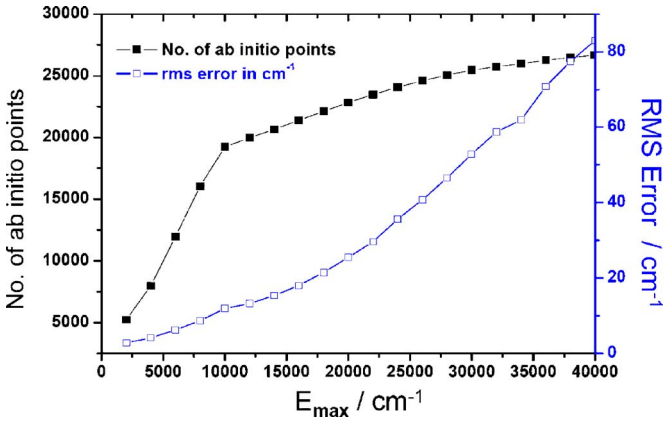

FIG. 1. (Color online) Total number of *ab initio* points and root mean square fitting error as a function of energy up to E_{max}, relative to the global minimum.

and 15 bohrs, and finally one at 50 bohrs and one at 100 bohrs. At each OO distance, between 300 and 2000 monomer geometries were selected for a total of 15 000 configurations. Roughly 3000 additional data points were generated at configurations where the energy is less than 2000 cm^{-1} (relative to the minimum on the fit) and then 1800 additional energies were done to yield a PES that gave a stable quantum diffusion Monte Carlo (DMC) zero-point energy (ZPE) in full dimensionality. The final data set for this previous PES consisted of 19 805 energies.

In the present work an additional 10 227 configurations were incorporated to improve the description of the potential at energies below 10 000 cm^{-1}. These additional energies were selected from a large set of geometries generated in vibrational configuration interaction and DMC calculations. The distribution of these energies is nearly uniform in the range of 0–10 000 cm^{-1}. As in the previous work, the standard counterpoise correction was applied to approximately correct the basis-set-superposition error, even though the correction is relatively small, i.e., of the order of 10–60 cm^{-1}. Of the 30 082 configurations 5235 are below 2000 cm^{-1} and 19 754 are below 10 000 cm^{-1}.

The *ab initio* energies were fit using linear least squares in terms of a special set of polynomials as described previously and in detail in our application to the PES for the protonated water dimer, $H^+(H_2O)_2$.[14] In brief the fit is performed in terms of the 15 variables $x_{ij}=e^{-r_{ij}/3}$ for the main polynomial, denoted by p, and $y_{ij}=e^{-r_{ij}}/r_{ij}$ for the two-body short-range polynomial, denoted by q, and where r_{ij} is the ijth internuclear distance. The polynomial p is of total degree 7 and q is a quartic. The polynomial p is expanded on a basis in which each element is invariant under the complete permutation symmetry group of the molecule. The basis is truncated at total degree 7 and is complete for polynomials up to that total degree. The expansion coefficients are determined by a weighted least squares fit to the *ab initio* data, and the weight of a data point with energy E relative to the global minimum was $(E_0/(E_0+E))^2$ with E_0 set to 0.01 hartree. In total, there are 5227 terms in the expression for the PES.

The fitted potential energy surface describes dissociation to two monomers and does so with full permutational symmetry. The energies of interest in the present study are much below what is required for dissociation of a H_2O monomer or for hydrogen exchange between the two monomers. Nevertheless, the complete permutational symmetry is a correct property of the physical potential, and by building this property into the basis we achieve a significant economy in the size of the basis.

The fitting rms error as a function of the energy cutoff is shown in Fig. 1. As seen, at 2000, 6000, 10 000, 20 000 and 40 000 cm^{-1}, the errors are 2.0, 5.8, 11.7, 25.4, and 83.0 cm^{-1}, respectively. To test the accuracy of the fit beyond the analysis of the rms fitting error, we checked the predictive accuracy of the fit by comparing it to additional *ab initio* energies not included in the fit. These were done for 16 values of the O–O stretch, and the rms error is 11 cm^{-1}; for 21 points along free O–H bond stretches and the rms error is 22 cm^{-1}; for randomly generated geometries from DMC walkers for 49 points below 8 000 cm^{-1} and the rms error is 9.8 cm^{-1}; and 34 cm^{-1} for 48 points between 8000 and 25 000 cm^{-1}. (Note that these rms errors for predictions are roughly a factor of 2 smaller than for the HBB0 potential.[11])

Now we present a number of properties of the HBB PES. Ten fully relaxed stationary points were located, and the energies, geometries, and harmonic frequencies are given in Tables I and II. Compared to previous work,[11] the barrier heights of SP2–SP10 differ by only 0–5 cm^{-1}. Changes of the monomer equilibrium geometry are less than 0.0001 Å and 0.06°, while most intermonomer parameters change by 0.002–0.010 Å for r_{O-O} and 0°–2° for angles. For monomer bending and OH stretch modes the harmonic frequencies vary by 0–4 cm^{-1}. For intermonomer normal mode frequencies, 5–16 cm^{-1} differences are found for rocking/wagging and OO stretches; these intermolecular frequencies changed more as they are more sensitive to small changes in the PES. Thus, the level of agreement between HBB and the benchmark single-point calculations of Tschumper *et al.*[15] remains about the same or is slightly improved compared to HBB0.[11]

The HBB PES dissociates to two equivalent H_2O molecules with dissociation energy D_e of 1665.82 cm^{-1} (19.9 kJ/mol). This value compares well with the benchmark *ab initio* value of 21.0 kJ/mol.[15] The H_2O equilibrium properties are as follows: $r_{OH}=0.9615$ Å, $\angle HOH=104.2°$ and the barrier to linearity is 11 116 cm^{-1} with $r_{OH}=0.9381$ Å. Harmonic frequencies are 1642, 3810, and 3921 cm^{-1} and the "exact" vibrational ZPE and corresponding fundamentals are 4615, 1595, 3638, and 3737 cm^{-1}, respectively. The DMC ZPE is 9856 ± 3 cm^{-1} and, thus, D_0 is 1040 cm^{-1} for $(H_2O)_2$, i.e., 12.44 kJ/mol. This value is slightly below the value of D_0, 12.93 kJ/mol, obtained from the VRT(ASP-W) potential fitted to the measured VRT levels.[16] The zero-point averaged structure of $(H_2O)_2$ is as follows: $r_{OO}=3.03\pm0.02$ Å, the bridging r_{OH} of the donor is 0.990 Å, the donor free r_{OH} is 0.985 Å, the acceptor r_{OH} is 0.987 Å, and the $\angle HOH=104.0°$. A discussion of previous calculations of the dissociation properties of $(H_2O)_2$ was given in Ref. 11 and so is not repeated here.

As the 6D exact quantum computations were run with water monomer geometries fixed at the isolated monomer equilibrium geometry it is of interest to compare the geom-

TABLE I. Energy (E in cm^{-1}), dipole moment (a.u.), and geometry (Å, deg) of ten stationary points (SP) on the HBB potential.

				Intramonomer geometry						Intermonomer geometry						
SP	Sym.	E	Dipole	$R_{O_1H_1}$	$R_{O_1H_2}$	$R_{O_2H_3}$	$R_{O_2H_4}$	$\angle H_1O_1H_2$	$\angle H_3O_2H_4$	$R_{O_2H_2}$	$\angle O_1H_2O_2$	$\angle H_3O_2O_1$	$\angle H_4O_2O_1$	$\tau_{O_2H_2O_1H_1}$	$\tau_{O_3H_2O_1H_2}$	$\tau_{O_4H_2O_1H_2}$
CsMin	C_s	0.0	1.01795	0.9607	0.9675	0.9622	0.9622	104.50	104.61	1.9778	171.70	109.57	109.57	180.00	122.88	−122.88
SP2	C_1	161.4	1.30423	0.9607	0.9670	0.9623	0.9617	104.58	104.62	2.0233	167.64	103.29	126.80	158.44	170.09	50.04
SP3	C_s	198.5	1.33016	0.9606	0.9663	0.9616	0.9611	104.54	105.06	2.0046	166.95	110.61	144.33	180.00	180.00	0.00
SP4	C_i	244.0	0.00000	0.9612	0.9644	0.9612	0.9644	104.83	104.83	2.2955	115.07	130.92	47.03	−132.80	109.54	180.00
SP5	C_2	329.3	0.64278	0.9609	0.9640	0.9609	0.9640	104.95	104.95	2.3040	112.14	145.85	49.35	−154.12	−118.90	−167.59
SP6	C_{2h}	348.1	0.00000	0.9606	0.9636	0.9606	0.9636	105.08	105.08	2.3095	109.90	156.22	51.14	180.00	180.00	180.00
SP7	C_s	603.0	1.43363	0.9618	0.9624	0.9624	0.9624	104.54	101.96	3.1619	70.27	53.37	53.37	180.00	−104.51	104.51
SP8	C_{2h}	1181.8	0.00000	0.9621	0.9621	0.9621	0.9621	103.19	103.19	3.1062	92.64	70.39	70.39	−63.29	180.00	67.41
SP9	C_{2v}	590.2	1.61833	0.9623	0.9623	0.9619	0.9619	101.65	104.48	2.5322	112.04	127.76	127.76	0.00	−90.00	90.00
SP10	C_{2v}	898.3	1.59506	0.9618	0.9618	0.9619	0.9619	101.93	104.07	2.6788	112.84	127.96	127.96	0.00	0.00	180.00

etries and energies of the fully relaxed barriers with rigid monomer barriers, obtained with constrained optimizations. These are given in Table III where it is seen that the rigid monomer barriers agree very well with the fully relaxed ones. We will discuss the small differences in more detail after the results of the tunneling splitting calculations are presented in the next section.

Finally, we note that the permutationally invariant dipole moment surface reported previously has been updated using the larger data set MP2/aug-cc-pVTZ dipole values. As previously, the new DMS dissociates correctly to the monomer DMS. Total fitting rms errors along x-, y-, and z-dipole components are 0.016, 0.009, and 0.009 a.u., respectively. The error along the x direction is bigger just because we have aligned the O–O axis along the x axis. Comparing to the previous DMS, the fitting accuracy is improved by 20%. Dipole moments on ten characteristic SP structures have been checked (see Table I). Changes of dipole moments on ten SPs are only 0.0–0.1%, compared with those reported previously.[11] The values of the MP2-based DMS at the $(H_2O)_2$ global minimum and the H_2O monomer equilibrium geometry are 1.02 and 0.729 a.u., respectively, slightly smaller than the benchmark values of 1.06 and 0.757 a.u. of Tschumper *et al.*[15] To obtain the vibrationally averaged dipole moment rigorously is nontrivial. We have estimated this based on a DMC calculation and obtain 1.07 a.u. with an uncertainly of roughly ±0.01 a.u.

III. VIBRATION-ROTATION TUNNELING SPECTRUM OF THE WATER DIMER

Without breaking any of the chemical bonds, the water dimer has access to eight equally deep minima in the global potential energy surface that correspond to eight equivalent equilibrium structures related by interchanging identical nuclei. These interchange operations are called "feasible" because they become possible by quantum mechanical tunneling through the energy barriers between the equivalent minima, which leads to observable splittings in the spectrum. Combined with inversion, they generate the permutation-inversion (PI) symmetry group G_{16} of the water dimer. The VRT levels of this dimer, split by tunneling, are commonly labeled with the irreducible representations (irreps) $A_1^{\pm}$, $B_1^{\pm}$, $A_2^{\pm}$, $B_2^{\pm}$, and $E^{\pm}$ of G_{16}. Our computation of these VRT levels of the water dimer involves a fully coupled treatment in all six intermolecular degrees of freedom, similar to a coupled-channel scattering calculation.[12] The monomers are frozen at their calculated isolated molecule equilibrium geometry. It was demonstrated in several papers that the resulting water dimer VRT levels, through a comparison with the high accuracy experimental data available,[1–9] provide an extremely sensitive test of water pair potentials. Here, we apply this test to the *ab initio* HBB potential described in this paper, as well as to its predecessor HBB0.[11]

The formalism is explained in detail in Ref. 12. An angular basis of symmetric rotor functions $D_{mk}^{(j)*}$ is used for the internal rotation of each of the monomers A and B; it was truncated at maximum values of j_A and j_B equal to 11 for H_2O dimer and 12 for D_2O dimer. It was found[12] that the

TABLE II. $(H_2O)_2$ harmonic frequencies (cm^{-1}) of ten stationary points (SP) on the HBB potential.

SP	Intermonomer normal modes						Intramonomer normal modes					
CsMin	123	137	142	177	344	600	1646	1665	3736	3806	3892	3912
SP2	91i	125	160	166	378	493	1647	1671	3747	3808	3896	3914
SP3	153i	76i	110	161	353	437	1644	1669	3762	3815	3898	3924
SP4	128i	113	148	184	356	549	1640	1647	3784	3795	3902	3905
SP5	120i	58	99	159	325	482	1634	1657	3795	3795	3909	3912
SP6	131i	81i	76i	154	366	386	1634	1655	3798	3803	3913	3921
SP7	203i	62i	131	159	267	412	1638	1654	3803	3817	3908	3914
SP8	227i	162i	125i	80	247	358	1652	1653	3805	3812	3904	3910
SP9	220i	50	121	159	203	417	1638	1659	3804	3821	3904	3916
SP10	238i	178i	87	96	162	327	1642	1660	3802	3828	3913	3918

VRT levels were sufficiently well converged at these values to reliably extract even the smallest tunneling splittings. Symmetric rotor functions $D_{MK}^{(J)*}$ were also used for the overall rotation of the complex with quantum numbers J, the total angular momentum of the complex, M, the projection of this angular momentum on a space-fixed axis, and K, the projection on the dimer z axis. The latter axis coincides with the vector **R** that points from the center of mass of monomer A to that of monomer B. The quantum numbers J and M are exact quantum numbers. Also, K becomes a good quantum number because we neglected the off-diagonal Coriolis coupling between the internal angular momenta $\mathbf{j}_A$, $\mathbf{j}_B$ and the overall angular momentum **J**; this coupling leads only to a minute asymmetry doubling of the water dimer levels. For the radial coordinate R, the length of the vector **R**, we used a discrete variable representation (DVR) with three contracted DVR functions obtained by using a one-dimensional radial cut through the equilibrium geometry in the six-dimensional potential surface, see Ref. 12. It was checked[17] that this radial basis, although small, gives well converged results. The adaptation of the basis to the different irreps of the PI group G_{16} considerably simplifies the calculations.

The quantities that we use to characterize the spectra are the same as used by the experimentalists and are defined in Refs. 6–9. For $K=0$, the origins o_1 and o_2 are the average energies of the $J=0$ levels of A_1^+ and B_1^+ symmetries and of A_2^- and B_2^- symmetries, respectively. The end-over-end rotational constant $B+C$ for $K=0$ was obtained as the difference between levels with $J=1$ and $J=0$. For $K>0$, the levels occur in degenerate pairs, $A_1^{\pm}$, $B_1^{\mp}$ and $A_2^{\pm}$, $B_2^{\mp}$, due to our neglect of the off-diagonal Coriolis coupling. The origins o_1 and o_2 were obtained from averaging the A_1^+ and B_1^+ levels and the A_2^- and B_2^- levels, respectively. Then, according to the convention used by experimentalists, the origins were calculated from the levels with the lowest value of J $(=K)$ by subtraction of $(B+C)K/2$. The value of $B+C$ for $K=1$ was obtained from the difference between $K=1$ levels with $J=2$ and $J=1$. The much larger rotational constant A for rotation about the prolate axis (nearly coinciding with the vector **R**) was obtained as the difference between the $K=1$ and $K=0$ averages $(o_1+o_2)/2$.

The largest tunneling splitting, denoted by $a(K)$, is the so-called acceptor splitting, which is strongly K dependent. It is caused by an interchange of the two hydrogen atoms of the hydrogen bond acceptor monomer. The two corresponding minima in the potential surface are separated by the lowest energy barrier in the potential surface, saddle point SP2 in Tables I–III. The splitting $a(K)$ can be extracted from the (calculated or measured) spectra as the energy difference between the origins o_2 and o_1. The interchange splittings, denoted by i_1 and i_2, correspond to the interchange of the donor and acceptor molecules. The barrier that separates the two corresponding minima in the potential surface is saddle point SP4 in Tables I–III. These tunneling splittings can be extracted from the spectra as well: i_1 is the difference between the $B_1^{\pm}$ and $A_1^{\pm}$ levels and i_2 is the difference between the $B_2^{\mp}$ and $A_2^{\mp}$ levels. The $E^{\pm}$ levels that are slightly shifted with

TABLE III. Rigid monomer (RM) energy and barrier heights and intermonomer geometry (Å, deg) of ten stationary points found on the HBB potential. Fully relaxed barriers from Table I are also given for ease of comparison.

SP	Fully relaxed	RM Energy	RM barrier	$R_{O_2H_2}$	$\angle O_1H_2O_2$	$\angle H_3O_2O_1$	$\angle H_4O_2O_1$	$\tau_{O_2H_2O_1H_1}$	$\tau_{O_3H_2O_1H_2}$	$\tau_{O_4H_2O_1H_2}$
CsMin	0.0	9.1	0.0	1.9850	171.97	109.75	109.75	180.00	123.01	−123.01
SP2	161.4	168.6	159.5	2.0054	168.26	103.30	127.06	158.67	169.76	50.09
SP3	198.5	207.6	198.5	2.0107	167.26	111.05	144.75	180.00	180.00	0.00
SP4	244.0	251.8	242.7	2.3015	115.15	130.22	47.05	−132.39	110.35	180.00
SP5	329.3	338.0	328.9	2.3103	112.28	144.86	49.32	−153.45	−118.79	−167.61
SP6	348.1	358.1	349.0	2.3167	109.95	155.41	51.19	180.00	180.00	180.00
SP7	603.0	631.4	622.3	3.2769	65.21	53.68	53.68	180.00	−101.61	101.61
SP8	1181.8	1192.4	1183.3	3.1275	92.41	70.72	70.72	−63.29	180.00	66.54
SP9	590.2	625.1	616.0	2.5658	110.69	127.89	127.89	0.00	−90.00	90.00
SP10	898.3	925.8	916.7	2.7160	111.67	127.89	127.89	0.00	0.00	180.0

TABLE IV. VRT levels, tunneling splittings, and rotational constants (in cm^{-1}) of $(H_2O)_2$ calculated with the HBB0 potential in Ref. 11 and with the HBB potential in the present paper on the first and second rows, respectively. The numbers in parentheses are experimental values from Refs. 2, 3, and 7–9. The assigment of the intermolecular vibrations is given in Ref. 27. When it deviates from the earlier assignment according to Ref. 7, the latter is added in square brackets.

	o_1	o_2[a]	a	i_1	i_2	$B+C$	A
				Ground state (A')			
$K=0$	0.00	13.47	13.47	0.837	0.722	0.4117	
	0.00	13.33	13.33	0.745	0.641	0.4113	
	(0.00)	(11.18)	([b])	(0.752)	(0.651)	(0.4112)	
$K=1$	15.73	12.58	3.16	0.783	0.589	0.4116	7.42
	15.73	12.51	3.22	0.691	0.519	0.4112	7.46
	(14.39)	(11.66)	([b])	(0.705)	(0.541)	(0.4108)	(7.44)
				Donor torsion (A'')			
$K=0$	113.22	59.31	53.91	7.033	2.707	0.4149	
	116.10	60.77	55.33	6.356	2.383	0.4139	
		(64.52)			(2.54)		
$K=1$	84.65	91.08	6.43	1.349	3.809	0.4136	1.61
	85.87	92.68	6.81	1.039	3.318	0.4124	0.84
	(87.75)			(1.110)		(0.4083)	
				Acceptor wag (A')			
$K=0$	106.96	107.41	0.45	4.838	0.029	0.4116	
	107.00	106.13	0.87	3.915	0.005	0.4110	
	(107.93)	(108.89)	(0.96)	(2.951)	(0.017)	(0.4094)	
$K=1$	106.49	120.85	14.36	6.075	4.295	0.4128	6.49
	106.87	121.24	14.37	5.514	3.530	0.4123	7.50
	(109.98)	(123.56)	(13.58)	(5.238)	(3.412)	(0.4122)	(8.08)
				Acceptor twist (A'')			
$K=0$	129.54	113.55	15.99	1.358	9.753	0.4122	
	130.34	116.34	14.00	1.115	9.668	0.4117	
		(120.19)			(9.393)	(0.4138)	
$K=1$	139.70	133.23	6.48	4.427	5.552	0.4119	14.93
	141.32	135.23	6.09	4.285	5.657	0.4116	14.94
				Donor torsion overtone (A') [in-plane bend]			
$K=0$	124.86	148.70	23.84	9.151	1.608	0.4091	
	127.09	147.79	20.70	8.927	1.275	0.4078	
		(153.62)			(1.877)		
$K=1$	150.77	147.89	2.87	1.713	2.518	0.4055	12.55
	149.88	147.10	2.78	1.449	1.676	0.4034	11.05
				Stretch (A')			
$K=0$	142.00	182.20	40.20	2.554	19.604	0.4093	
	140.16	183.84	43.67	2.719	19.173	0.4088	

[a]Since the experimental values of o_2 were given relative to the ground state value of o_2, we added the estimated ground state acceptor splitting $a(K=0)=11.18$ cm^{-1} (Ref. 12) to all experimental values.
[b]Acceptor splitting $a(K=0)+a(K=1)=16.63$ and $16.55 cm^{-1}$ (calculated) and 13.92 cm^{-1} (experimental).

respect to the average energies of the $A_1^{\pm}$ and $B_1^{\pm}$ levels and the $A_2^{\pm}$ and $B_2^{\pm}$ levels by bifurcation tunneling through barrier SP9 have not been calculated.

The properties of the states with $K=0$ and $K=1$ calculated on the HBB0 and HBB potentials are listed and compared with the available experimental data in Tables IV and V for H_2O dimer and D_2O dimer, respectively. The dissociation energies D_0 for the H_2O rigid monomer dimer are 996.6 and 998.0 cm^{-1} for the HBB0 potential and the present HBB potential, respectively. For D_2O dimer, they are 1136.3 and 1137.8 cm^{-1}, respectively. The D_e values of these potentials with the monomers frozen at their equilibrium geometries are 1655.9 and 1656.0 cm^{-1}. The D_0 value may be compared with that from full 12-dimensional (12D) DMC calculations, which for the HBB potential is 1040 cm^{-1} for H_2O dimer. Harmonic calculations show that part of this binding energy is caused by a lowering of the monomer zero-point energy. The harmonic monomer ZPE in the H_2O dimer is

TABLE V. VRT levels, tunneling splittings, and rotational constants (in cm^{-1}) of $(D_2O)_2$ calculated with the HBB0 potential in Ref. 11 and with the HBB potential in the present paper on the first and second rows, respectively. The numbers in parentheses are experimental values from Refs. 1, 4–6, 8, and 9.

	o_1	o_2[a]	a	i_1	i_2	$B+C$	A
				Ground state (A')			
$K=0$	0.00	2.41	2.41	0.0485	0.0445	0.3711	
	0.00	2.37	2.37	0.0397	0.0364	0.3708	
	(0.00)	(1.77)	(1.77)	(0.0391)	(0.0361)	(0.3622)	
$K=1$	5.77	5.01	0.76	0.0443	0.0402	0.3711	4.19
	5.75	4.99	0.76	0.0362	0.0327	0.3708	4.19
	(5.36)	(4.74)	(0.62)	(0.0359)	(0.0331)	(0.3621)	(4.17)
				Donor torsion (A'')			
$K=0$	73.79	54.57	19.22	0.418	0.223	0.3710	
	75.58	55.88	19.70	0.301	0.174	0.3700	
	(75.38)	(59.59)	(15.81)	(0.328)	(0.203)	(0.3622)	
$K=1$	64.03	68.18	4.15	0.137	0.290	0.3700	1.92
	65.22	69.54	4.31	0.095	0.223	0.3691	1.65
	(68.27)	(71.81)	(3.54)	(0.132)	(0.257)	(0.3600)	(2.56)
				Acceptor wag (A')			
$K=0$	79.75	81.72	1.97	0.174	0.146	0.3701	
	78.95	80.38	1.44	0.145	0.110	0.3698	
	(82.64)	(84.40)	(1.77)	(0.131)	(0.112)	(0.3603)	
$K=1$	81.94	87.10	5.16	0.556	0.244	0.3709	3.79
	81.95	86.23	4.27	0.419	0.181	0.3705	4.43
	(85.57)	(89.56)	(4.00)	(0.398)	(0.168)	(0.3592)	(4.05)
				Acceptor twist (A'')			
$K=0$	88.44	84.90	3.55	0.449	0.918	0.3719	
	90.33	87.55	2.78	0.460	0.847	0.3717	
	(92.91)	(90.37)	(2.54)	(0.432)	(0.443)	(0.3665)	
$K=1$	94.73	91.42	3.30	0.499	0.699	0.3720	6.41
	96.17	93.82	2.35	0.504	0.651	0.3718	6.06
				Donor torsion overtone (A') (in-plane bend)			
$K=0$	96.88	129.37	32.49	0.950	1.786	0.3702	
	98.72	129.92	31.20	0.758	1.150	0.3686	
	(104.24)			(0.783)		(0.3632)	
$K=1$	121.41	113.33	8.08	0.672	0.005	0.3711	4.25
	122.78	114.42	8.36	0.451	0.028	0.3701	4.29
				Donor torsion+acceptor wag combination (A'')			
$K=0$	129.58	135.41	5.83	0.043	1.507	0.3710	
	129.30	136.10	6.80	0.001	1.165	0.3702	
				Stretch (A')			
$K=0$	130.28	140.93	10.66	3.082	2.159	0.3708	
	131.30	141.75	10.46	1.971	2.166	0.3677	

[a]Since the experimental values of o_2 were given relative to the ground state value of o_2, we added the experimental estimate (Ref. 5) for the ground state acceptor splitting $a(K=0)=53$ GHz$=1.7679$ cm^{-1} to all experimental values.

9328.8 cm^{-1}, while in the free monomers it is 9373.5 cm^{-1}, so the harmonic estimate of the monomer contribution to D_0 is 44.7 cm^{-1}. This lowering of the monomer ZPE is dominated by the large redshift of the OH stretch frequency of the hydrogen bonded donor OH group: 74 cm^{-1} in the harmonic calculations. Obviously, the monomer contribution to D_0 is absent from the (variational) 6D calculations with frozen monomers and D_e is decreased by about 9 cm^{-1} by freezing the monomers. Taking these differences into account shows that the numbers from the DMC and variational calculations are consistent.

The ground state tunneling levels of H_2O dimer and D_2O dimer calculated with the HBB potential are shown and compared with measured values in Figs. 2 and 3, respectively. The levels (origins o_1 and o_2) corresponding to the intermolecular vibrations of H_2O dimer and D_2O dimer are shown in

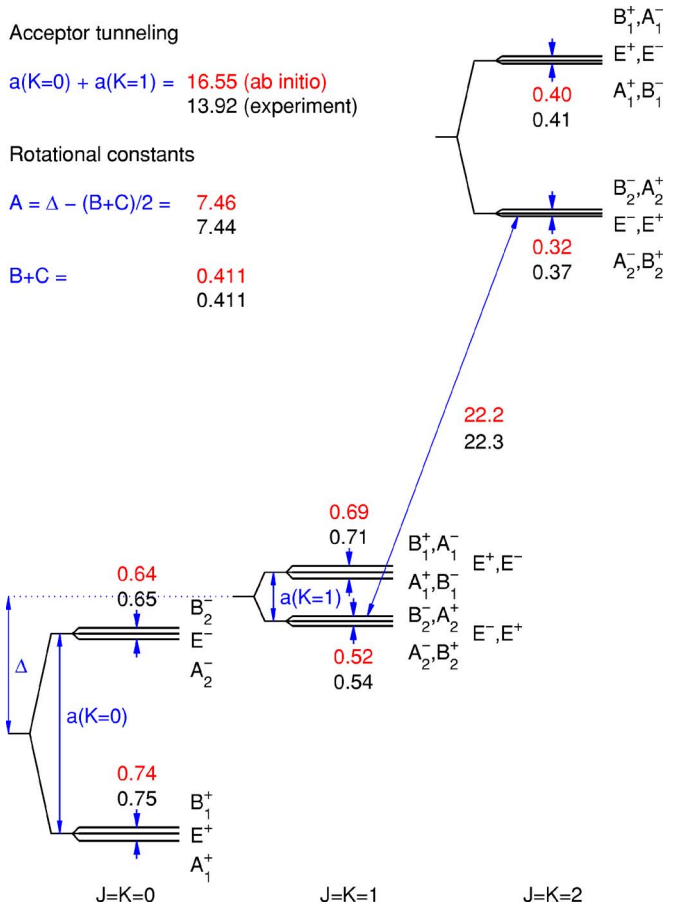

FIG. 2. (Color online) Ground state VRT levels of the H_2O dimer (in cm^{-1}) from converged calculations with the HBB *ab initio* potential, in comparison with experimental data (Refs. 2, 3, and 7) (lower numbers). The energies are drawn to scale.

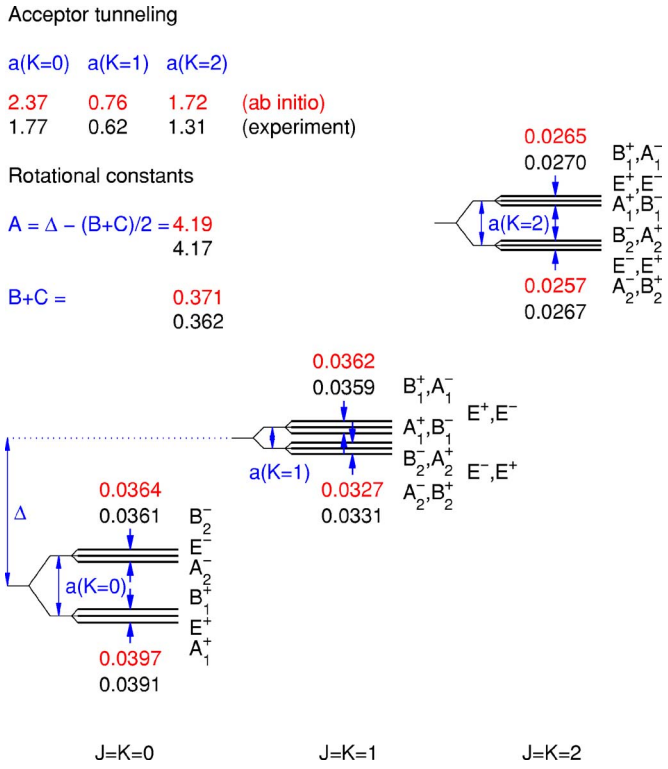

FIG. 3. (Color online) Ground state VRT levels of the D_2O dimer (in cm^{-1}) calculated from the HBB *ab initio* potential, in comparison with experimental data (Refs. 1 and 4–6) (lower numbers). The energies are drawn to scale, except for the small interchange splittings which are enlarged by a factor of 10.

Figs. 4 and 5, respectively. An overview of the quality of the VRT levels from the HBB0 and HBB potentials, relative to the experimental data, is given in Table VI. We may conclude that, for both potentials, the agreement with the experimental data is very good, and also that the HBB potential is still a substantial improvement over HBB0. The only quantity that is not well represented by both potentials is the acceptor splitting a_0+a_1. Calculations on the effects of monomer flexibility[18–20] have shown that this quantity $a(0)+a(1)$ decreases when the H_2O monomers are relaxed. It is striking in this respect, see Table VI, that the other pure *ab initio* potential that gives very good agreement with the experimental data, the 6D CC-pol potential,[10,17,21] gives practically the same deviation from experiment for $a(0)+a(1)$ as the HBB0 and HBB potentials. It is most probable that all of these potentials have reached the "rigid monomer limit" of the acceptor splitting. The other quantities appear to be much less sensitive to making the monomers flexible and their agreement with experiment is about equally good for all of the three potentials. There is one property for which the HBB potential performs by far the best: the interchange splittings i_1 and i_2. We discuss this point in more detail below.

For comparison, we also included in Table VI another recent *ab initio* potential, the TTM2.1 potential.[22] The VRT levels from this 12D potential, applied in 6D calculations with rigid monomers at their equilibrium geometry just as for the HBB potential, deviate much more from the experimental data than for the CC-pol, HBB0, and HBB potentials. Furthermore, we show results from the best of the family of 6D VRT(ASP-W) potentials, the VRT(ASP-W)III potential.[23] These potentials are based on *ab initio* calculations, while a number of the parameters in the analytic representation of the *ab initio* points were reoptimized by a fit of the VRT levels calculated for the D_2O dimer to the experimental data. It is remarkable that the best pure *ab initio* potentials to date, the HBB and CC-pol potentials, give results in better agreement with the experimental data than the VRT(ASP-W)III potential that was fitted to this data. Except for the acceptor splitting, of course, which—for the reason given in the previous paragraph—has not much to do with the quality of the potential, but rather with the fact that the monomers were frozen. We did not include the earlier *ab initio* potentials in our comparison, nor did we list any results obtained from the multitude of empirical potentials developed for simulations of liquid water. From such comparisons, discussed in Refs. 10, 17, and 21, it becomes clear that the empirical liquid water potentials are not at all capable of producing a water dimer VRT spectrum of reasonable quality. This is mostly because they are "effective" pair potentials that account implicitly for the important many-body forces in liquid water and ice. Furthermore, one can say that the accuracy of the older *ab initio* potentials is of a much lower level than that of the HBB0, HBB, and CC-pol potentials. Somewhat of an exception are the SAPT-5s (Ref. 24) and SDFT (Ref. 25)

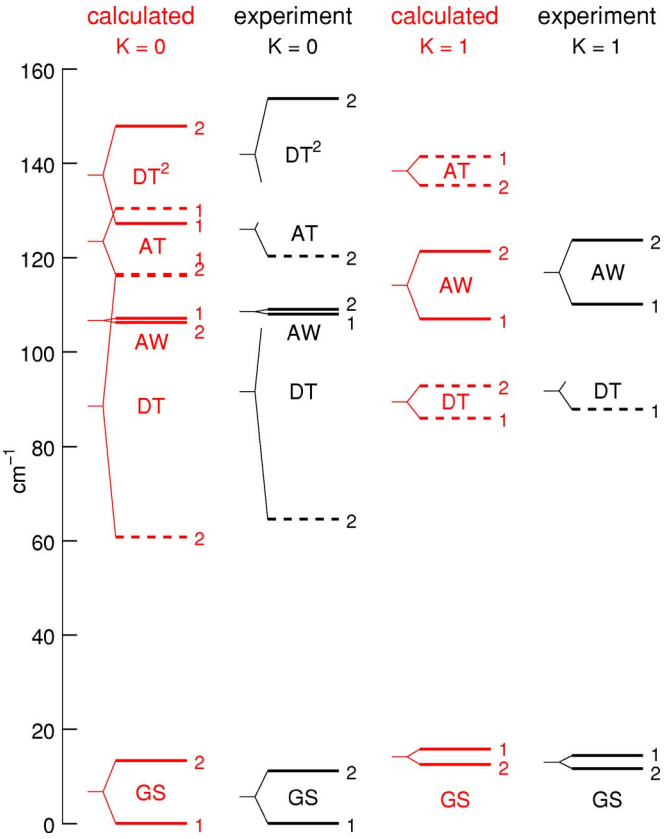

FIG. 4. (Color online) VRT levels of the H_2O dimer corresponding to the intermolecular vibrations, calculated from the HBB potential, in comparison with experimental data (Ref. 7). The levels 1 and 2 are the origins, o_1 and o_2, of the A_1,E_1,B_1 and A_2,E_2,B_2 levels, respectively. The abbreviations GS, DT, AW, and AT denote the ground state (A'), donor torsion (A''), acceptor wag (A'), and acceptor twist (A'') modes, following Refs. 7 and 27. Solid lines refer to A' symmetry, dashed lines to A'' symmetry, with respect to the point group C_s of the equilibrium structure. Experimental levels not shown have not been measured to date.

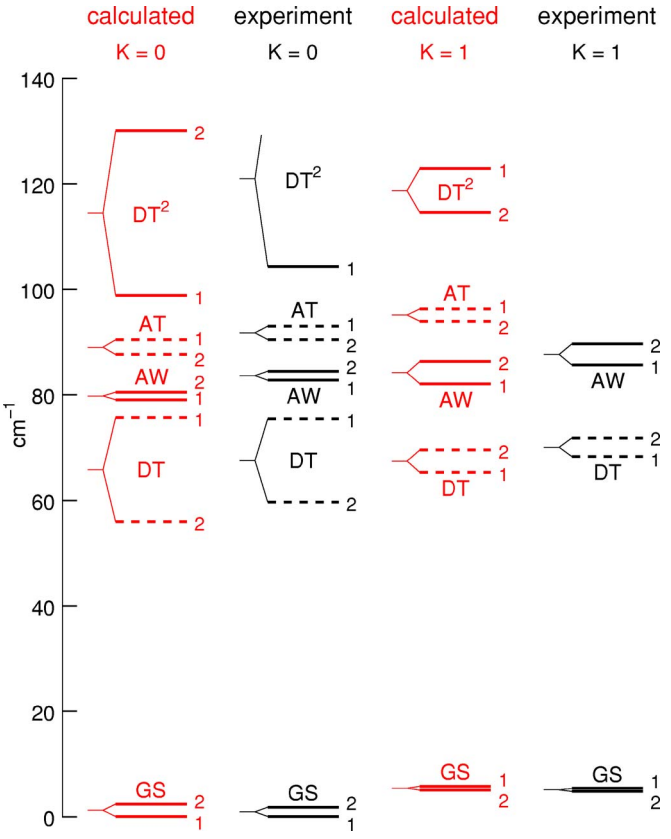

FIG. 5. (Color online) VRT levels of the D_2O dimer corresponding to the intermolecular vibrations, calculated from the HBB potential, in comparison with experimental data (Ref. 6). All symbols are explained in Fig. 4, except for DT^2 which denotes the donor torsion overtone (A') (Ref. 27). In Ref. 7 this mode was referred to as in-plane bend.

potentials, but even they are not of the same class as the HBB0, HBB, and CC-pol potentials.

Finally, let us discuss the amazingly good quality of the interchange splittings i_1 and i_2 obtained from the HBB potential. The donor-acceptor interchange process in the water dimer is hindered by a barrier in the potential surface that corresponds to saddle point SP4, see Tables I–III. The extremely good agreement with experiment for i_1 and i_2 indicates that the HBB potential describes this barrier very accurately. We may compare it to the CC-pol potential, which apart from i_1 and i_2, gives VRT levels of about the same quality as HBB. In the analytic representation of the CC-pol potential, special attention was given to obtaining the correct long range behavior, while its analytic form was chosen such that it is not too expensive in molecular dynamics calculations of liquid water. Both properties are essential for simulations of liquid water, but as a result of the latter property, the number of fit parameters was kept rather limited and the numerical accuracy of the fit is definitely lower than for the fit of HBB0 and HBB. Other aspects are important as well, though. Since the monomers were frozen in the 6D calculation of the dimer VRT levels, one may wonder what is the effect of relaxing the monomer geometries on the barriers through which the various tunneling processes occur. First, there is a direct effect: the barrier heights in the full 12D potential surface are not the same as in the 6D rigid mono-

TABLE VI. Root mean square relative percentage errors in various properties of H_2O and D_2O dimers from calculations with different potentials, compared with experimental data from Refs. 8 and 9 and references therein. The following properties are used in this analysis: ground state rotational constants A and $B+C$, ground state tunneling splittings $a(0)+a(1)$ (acceptor switch), i_1 and i_2 (donor-acceptor interchange), and frequencies of the intermolecular vibrations DT, AW, AT, and DT^2 for $K=0$.

Potential	Rotational constants	$a(0)+a(1)$	i_1,i_2	Vibrational frequencies
		H_2O dimer		
TTM2.1[a]	16	82	67	12
VRT(ASP-W)III[b]	6.6	0.1	55	6.9
CC-pol[c]	2.1	19	5.8	4.3
HBB0[d]	0.2	19	11	4.7
HBB	0.05	19	1.1	3.6
		D_2O dimer		
VRT(ASP-W)III[b]	2.2	11	64	4.5
CC-pol[c]	3.6	34	14	4.1
HBB0[d]	1.8	33	24	5.7
HBB	1.7	31	1.2	4.5

[a]References 10 and 22.
[b]References 8, 9, and 23.
[c]References 10, 17, and 21.
[d]Reference 11.

mer potential. It turns out, however, see Table III, that this effect is a minor one because the global minimum in the potential surface (or rather, the eight equivalent minima) is (are) lowered by relaxing the monomer geometries by about the same amount as the saddle points SP2 and SP4. A more important effect originates from the intramolecular vibrations. From harmonic calculations, see Table II, it is estimated that the SP2 barrier is effectively raised from 161.4 to 174.6 cm^{-1}, i.e., by 8%, by adding the monomer ZPEs calculated at the SP2 saddle point and at the minimum. This rise of the SP2 barrier partly explains why the acceptor tunneling splittings $a(K)$ will decrease when the monomers are made flexible. However, it should be mentioned that it is not just the height of the barrier that is important, also its shape and the amount of coupling between the different degrees of freedom are both important factors. For the SP4 barrier relevant for interchange tunneling, the effect of adding the monomer ZPE is considerably smaller: the harmonic estimate gives an increase of the barrier from 244.0 to 251.4 cm^{-1}, i.e., by 3%. Given that this effect is not completely negligible, however, it is remarkable that the HBB potential gives such accurate values of i_1 and i_2 in 6D rigid monomer calculations. Since the agreement with experiment is equally good for $(H_2O)_2$ and $(D_2O)_2$, it seems that the monomer vibrations do not play a role in the interchange tunneling splittings.

IV. SUMMARY AND CONCLUSIONS

We presented a full-dimensional global potential energy surface for the water dimer based on fitting roughly 30 000 electronic energies. These were obtained using the CCSD(T) method with an aug-cc-pVTZ basis. A corresponding dipole moment surface was also reported at the MP2 level of theory. These surfaces are both manifestly invariant with respect to all permutations of like atoms and both dissociate correctly to the monomer limit. Properties of these surfaces, especially the PES, were presented. Barriers to internal hydrogen bond rearrangements were presented for the fully relaxed potential and for the rigid monomer 6D case and found to be quite similar. This provides additional confidence in the reality of rigorous quantum calculations of intermolecular vibrational energies, tunneling splittings, and rotation constants done in the rigid monomer model, which were reported using this new PES, as well as with a previously published potential. Agreement with experiment obtained using the new PES was shown to be excellent and of the highest level reported to date. The remaining differences, in particular for the acceptor tunneling splitting, are ascribed mainly to the rigid monomer approximation made in the calculation of the water dimer VRT states, rather than to deficiencies in the PES. Additional calculations of the intramolecular vibrational energies and IR spectrum are underway[26] and work to build a model for water based on this PES is being planned.

ACKNOWLEDGMENTS

B.J.B. would like to thank the ONR (N00014–05–1–0460), J.M.B. would like to thank the NSF (CHE-0446527), R.E.A.K. and J.T. would like to thank the NERC and EPSRC through the CAVIAR consortium for funding.

[1] E. Zwart, J. J. ter Meulen, and W. L. Meerts, Chem. Phys. Lett. **173**, 115 (1990).
[2] E. Zwart, J. J. ter Meulen, W. L. Meerts, and L. H. Coudert, J. Mol. Spectrosc. **147**, 27 (1991).
[3] G. T. Fraser, Int. Rev. Phys. Chem. **10**, 189 (1991).
[4] E. N. Karyakin, G. T. Fraser, and R. D. Suenram, Mol. Phys. **78**, 1179 (1993).
[5] J. B. Paul, R. A. Provencal, and R. J. Saykally, J. Phys. Chem. A **102**, 3279 (1998).
[6] L. B. Braly, J. D. Cruzan, K. Liu, R. S. Fellers, and R. J. Saykally, J. Chem. Phys. **112**, 10293 (2000).
[7] L. B. Braly, K. Liu, M. G. Brown, F. N. Keutsch, R. S. Fellers, and R. J. Saykally, J. Chem. Phys. **112**, 10314 (2000).
[8] F. N. Keutsch, N. Goldman, H. A. Harker, C. Leforestier, and R. J. Saykally, Mol. Phys. **101**, 3477 (2003).
[9] F. N. Keutsch, L. B. Braly, M. G. Brown, H. A. Harker, P. B. Petersen, C. Leforestier, and R. J. Saykally, J. Chem. Phys. **119**, 8927 (2003).
[10] R. Bukowski, K. Szalewicz, G. C. Groenenboom, and A. van der Avoird, Science **315**, 1249 (2007).
[11] X. Huang, B. J. Braams, and J. M. Bowman, J. Phys. Chem. A **110**, 445 (2006).
[12] G. C. Groenenboom, P. E. S. Wormer, A. van der Avoird, E. M. Mas, R. Bukowski, and K. Szalewicz, J. Chem. Phys. **113**, 6702 (2000).
[13] H.-J. Werner, P. J. Knowles, R. Lindh, M. Schütz, P. Celani, T. Korona, F. R. Manby, G. Rauhut, R. D. Amos, A. Bernhardsson *et al.*, MOLPRO, version 2002.6, a package of *ab initio* programs, 2003, see http://www.molpro.net.
[14] X. Huang, B. J. Braams, and J. M. Bowman, J. Chem. Phys. **122**, 044308 (2005).
[15] G. S. Tschumper, M. L. Leininger, B. C. Hoffman, E. F. Valeev, H. F. Schaefer III, and M. Quack, J. Chem. Phys. **116**, 690 (2002).
[16] F. N. Keutsch and R. J. Saykally, Proc. Natl. Acad. Sci. U.S.A. **98**, 10533 (2001).
[17] R. Bukowski, K. Szalewicz, G. C. Groenenboom, and A. van der Avoird, "Polarizable interaction potential for water from coupled cluster calculations. I. Analysis of dimer potential energy surface," J. Chem. Phys. (accepted).
[18] C. Leforestier, F. Gatti, R. S. Fellers, and R. J. Saykally, J. Chem. Phys. **117**, 8710 (2002).
[19] Y. Scribano, N. Goldman, R. J. Saykally, and C. Leforestier, J. Phys. Chem. A **110**, 5411 (2006).
[20] K. Szalewicz, G. Murdachaew, R. Bukowski, O. Akin-Ojo, and C. Leforestier, in *Lecture Series on Computer and Computational Science: ICCMSE 2006*, edited by G. Maroulis and T. Simos (Brill Academic, Leiden, 2006), Vol. 6, pp. 482–491.
[21] R. Bukowski, K. Szalewicz, G. C. Groenenboom, and A. van der Avoird, "Polarizable interaction potential for water from coupled cluster calculations. II. Applications to dimer spectra, virial coefficients, and simulations of liquid water," J. Chem. Phys. (accepted).
[22] G. S. Fanourgakis and S. S. Xantheas, J. Phys. Chem. A **110**, 4100 (2006).
[23] N. Goldman, R. S. Fellers, M. G. Brown, L. B. Braly, C. J. Keoshian, C. Leforestier, and R. J. Saykally, J. Chem. Phys. **116**, 10148 (2002).
[24] E. M. Mas, R. Bukowski, K. Szalewicz, G. C. Groenenboom, P. E. S. Wormer, and A. van der Avoird, J. Chem. Phys. **113**, 6687 (2000).
[25] R. Bukowski, K. Szalewicz, G. C. Groenenboom, and A. van der Avoird, J. Chem. Phys. **125**, 044301 (2006).
[26] Y. Wang, S. Carter, B. J. Braams, and J. M. Bowman, "MULTIMODE quantum calculations of intermolecular vibrational energies of the water dimer and trimer using *ab initio*-based potential energy surfaces," J. Chem. Phys. (submitted).
[27] M. J. Smit, G. C. Groenenboom, P. E. S. Wormer, A. van der Avoird, R. Bukowski, and K. Szalewicz, J. Phys. Chem. A **105**, 6212 (2001).